Atomic number measurement precision of spectral decomposition methods for CT

B. J. Heismann, Computed Tomography Division, Siemens Medical Solutions

***Abstract*– We have investigated the classical attenuation decomposition and base material decomposition CT algorithms invented by Alvarez and Macovski in 1976 for their ability to provide quantitative atomic number *Z* of a given attenuator. For this purpose we have generated attenuation functions of the elements from *Z* = 1 to *Z* = 20 from measured attenuation data. We have fitted these functions to two sets of base functions: 1. the Photoelectric absorption + Klein-Nishina scattering model and 2. the effective bone and water attenuator model. The results indicate model mismatches in the range of *ΔZ* = ±0.5 for the base material decomposition and *ΔZ* = ±0.7 for the attenuation decomposition.**

I. INTRODUCTION

In 1976, Alvarez and Macovski [1,2] proposed dual-energy CT as a method to further increase the contrast resolution. Their *attenuation decomposition* algorithm determines the coefficients of photoelectric absorption and Compton scatter attenuation by two CT measurements with different tube voltages. They also proposed the *base-material decomposition* which uses alternate sets of base functions, e.g. the attenuation functions of water and bone material.

The decomposition methods have been used in a number of studies; see e.g. the early works [3-7].

In this paper we simulate the precision of the Alvarez method to reconstruct the atomic number of known attenuators. This defines the lower systematical error limit for its quantitative results.

II. THEORY

The governing equation for polychromatic X-ray measurements of intensity *I* is

$$I = \int_E S(E) D(E) \exp\left(- \int_{\{P\}} \kappa(E,\vec{r})\, d\vec{r} \right) dE \qquad (1)$$

with $S(E)$: Primary X-ray tube spectrum, $D(E)$: detector absorption probability and $\kappa(E,r)$: spectral attenuation coefficient. The integral is taken along the path *{P}* of the x-ray beam.

For the effective attenuation coefficient μ this means

$$\mu = \ln\left(\frac{I_0}{I}\right) = \ln \int_E w(E) \exp\left(- \int_{\{P\}} \kappa(E,\vec{r})\, d\vec{r} \right) dE \qquad (2)$$

with the spectral weighting function

$$w(E) = \frac{S(E)D(E)}{\int_E S(E)D(E)dE}. \qquad (3)$$

The basic idea of Alvarez and Macosvki [1] is to write $\kappa(E, \mathbf{r})$ as a sum of two energy-dependent base functions

$$\kappa(E,\vec{r}) = \kappa_1(E,\vec{r}) + \kappa_2(E,\vec{r}). \qquad (4)$$

For the original attenuation decomposition they proposed κ_1 = Photoelectric absorption modelled by a_1 x E^{-3} and κ_2 = Compton scattering attenuation given by a_2 x the Klein-Nishina function. For the modified base material decomposition [2] the cross-sections of two base materials are taken. Efficient sets of materials have been investigated [3-7], in this paper we use κ_1 = equiv. H_2O and κ_2 = equiv. CaHAP (bone mineral).

In both cases the integration over *E* in (1) can be performed and we obtain line integrals over coefficients to be recovered by e.g. a filtered back-projection.

III. MATERIALS AND METHODS

We have taken the elemental attenuation spectra $\kappa(E,Z)$ for $Z = 1$ to $Z = 20$ from precise measurements [8-9]. We performed a least-squares fit of (4) with

$$\kappa_{AC}(E,Z) = \frac{a_1}{E^3} + a_2 f_{Klein-Nishina}(E) \qquad (5)$$

in case of the attenuation decomposition and

$$\kappa_{BM}(E,Z) = b_1 \kappa_{H2O}(E) + b_2 \kappa_{CaHAP}(E) \qquad (6)$$

in case of the base material decomposition. The resulting coefficients (a_1, a_2) and (b_1, b_2) were transformed to atomic number data by

$$Z_{AC} = c \cdot (a_1 / a_2)^{1/n}, n \approx 3, c = \text{const.} \qquad (7)$$

for the attenuation decomposition and

Author to whom correspondence should be directed, bjoern.heismann@siemens.com

$$Z_{BM} = \left(b_1 Z_{H2O}{}^{n} + b_2 Z_{CaHAP}{}^{n}\right)^{1/n} \qquad (8)$$

for the base material decomposition. Equations (7, 8) follow from the approximate analytic descriptions of the photo effect absorption and Compton attenuation, see e.g. [1], (4-5). Note that the constant *c* in (7) can be determined by calculation or the fit of Z_{AC} to the expected data in one reference point.

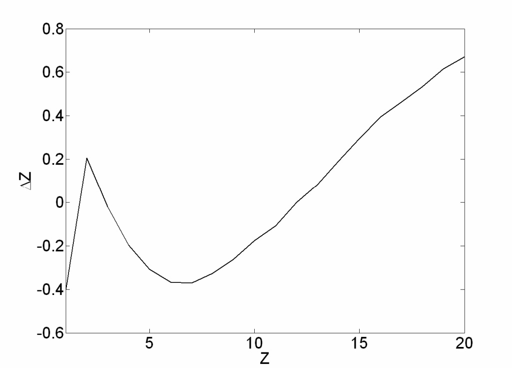

Fig. 1. Deviations of the reconstructed atomic number for the attenuation decomposition according to (5, 7).

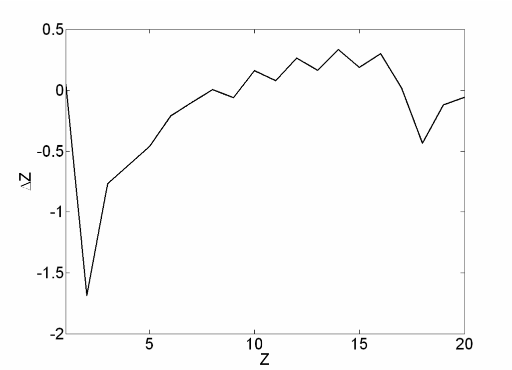

Fig. 2. Deviations of the reconstructed atomic number for the base material decomposition with water and bone as base materials according to (6, 8).

IV. RESULTS

Fig. 1, 2 and Table 1 summarize the results. We obtain the following results:

1. Attenuation decomposition

Figure 1 shows the deviation of the reconstructed effective Z_{AC} values according to (7) to the expected values *Z*. The calibrating factor *c* has been normalized to yield a precise *Z* = 12 mid-value in our case. For the typical diagnostic CT range between fat and iodine enhanced blood *Z* = ~6 … ~18, the systematic deviation is up to 0.7. In this region the error monotonously increases with distance from the normalization point *Z* = 12.

2. Base material decomposition

Figure 2 shows the reconstructed effective Z_{BM} value according to (8). For *Z* = ~7.5 and *Z* = ~15.9 the deviation is minimal since here the base materials match the material to be represented. We can recover *Z* with a systematic error of up to +/- 0.5 for the diagnostic range of *Z* = 6 … 18.

When comparing Figs. 1 and 2, the base material decomposition yields a better reconstructed *Z* of the attenuator material. The main reason for this is the rather significant deviation of the modeled E^{-3} dependency for the photo-effect in (5), see also [10]. The water plus bone superposition is more precise, especially in the range from *Z* = 7 to *Z* = 16, where the typical systematic error is around 0.3.

It should be noted that the observed deviations in the Z reconstruction are a source of artifacts in spectrally decomposed CT imaging. Simulations on this will be presented elsewhere.

TABLE 1
Results of the reconstructed Z_{AC}, Z_{BM} (7-8) for the range *Z* = 5 to *Z* = 18.

Z	Z_{AC}	Z_{BM}	*Z*	Z_{AC}	Z_{BM}
5	4.69	4.53	12	12.00	12.26
6	5.63	5.79	13	13.08	13.16
7	6.62	6.90	14	14.19	14.33
8	7.67	8.01	15	15.29	15.19
9	8.74	8.94	16	16.39	16.29
10	9.82	10.16	17	17.46	17.02
11	10.89	11.08	18	18.53	18.88

V. SUMMARY

The systematic precision of atomic number measurements in spectral CT decomposition methods has been analyzed. In the diagnostic CT region from *Z* = 6 (fat) to *Z* = 18 (calcifications and iodine enriched blood) we find a maximal systematic error of $\Delta Z = \pm 0.5$ for the base material decomposition and $\Delta Z = \pm 0.7$ for the attenuation decomposition.

REFERENCES

[1] R.E. Alvarez. A. Macovski, Energy-selective reconstructions in X-ray computerized tomography, Phys. Med Biol. 21(5):733-44 (1976)
[2] A. Macovski, R.E. Alvarez. J.L. Chan. J.P. Stonestrom. L.M. Zatz, Comp. Biol. Med. 6(4):325-36 (1976)
[3] W.R. Brody, G. Butt, A. Hall, and A. Macovski, Med. Phys. 8, 354 (1981)
[4] M. Chen, R.E. Alvarez and A. Macovski, IEEE Trans. Nucl. Sci 23, 551 (1976)
[5] A.L. Lehmann, R.E. Alvarez, A. Macovski, W.R. Brody, N.J. Pelc, S.J. Riederer, and A.L. Hall, Med. Phys. 8, 659 (1981)
[6] R.A. Brooks, J. Comput. Assist. Tomogr. 1, 487 (1977)
[7] J.B. Weaver, A.L. Huddleston, Attenuation coefficients of body tissues using principal-components analysis, Med. Phys. 12(1) 40-45 (1985)
[8] Tables and Graphs of Atomic Subshell and Relaxation Data Derived from the LLNL Evaluated Atomic Data Library (EADL), Z=1-100, S.T.Perkins, D.E.Cullen, M.H.Chen, J.H.Hubbell, J.Rathkopf, J.Scofield, UCRL-50400, Vol.30 (1991)
[9] Tables and Graphs of Photon-Interaction Cross Sections from 10 eV to 100 GeV, Derived from the LLNL Evaluated Photon Data Library (EPDL), UCRL-50400, Vol. 6, Rev. 4, D.E. Cullen, M H Chen, J H Hubbell, S.T. Perkins, E F Plechaty, J A Rathkopf, J H Scofield, Lawrence Livermore National Laboratory (1989)
[10] J.H. Hubbell, Natl. Bur. Stand. (U.S.) Publication No. NSRDS-NBS 29 (1969)